Synthesis of Luminescent Thin-Film CdSe/ZnSe Quantum Dot Composites Using CdSe Quantum Dots Passivated with an Overlayer of ZnSe

Michal Danek,[†,§] Klavs F. Jensen,*[,‡] Chris B. Murray,[†,⊥] and Moungi G. Bawendi[†]

Departments of Chemistry, Chemical Engineering and Materials Science and Engineering, Massachusetts Institute of Technology, Cambridge, Massachusetts 02139-4307

Received July 10, 1995. Revised Manuscript Received October 5, 1995[⊗]

Electronic and chemical passivation of CdSe nanocrystals (quantum dots) has been achieved with a thin ZnSe overlayer grown in solution from trioctylphosphine selenide and diethylzinc. Layered particles with a [ZnSe/CdSe] ratio ranging from 0 to ∼5.0 were prepared and characterized by optical absorption spectroscopy, photoluminescence, high-resolution transmission electron microscopy, Auger electron spectroscopy, and X-ray scattering. The overgrown particles were crystalline and displayed band-edge absorption and emission characteristic of the initial CdSe nuclei. Thin-film quantum dot composites incorporating bare and overcoated CdSe nanocrystals in a ZnSe matrix were synthesized by electrospray organometallic chemical vapor deposition (ES-OMCVD). The photoluminescence spectra of the composites with bare CdSe dots were dominated by broad deep-level emission and the photoluminescence yield deteriorated with increasing deposition temperature. In contrast, the composites incorporating the overcoated dots showed sharp band-edge emission. The presence of a preformed ZnSe layer resulted in a dramatic enhancement of the band-edge photoluminescence yield (by 2 orders of magnitude). The photoluminescence properties of composites with the passivated dots were insensitive to deposition temperature over the range studied.

Introduction

Semiconductor nanocrystals (quantum dots) display unique optical properties as a result of three-dimensional (3D) carrier confinement effects.[1] Specifically, the high luminescence yield and the potential of adjusting emission and absorption wavelengths by selecting the nanocrystal size make these materials attractive for applications in optoelectronics and nonlinear optics. CdSe/ZnSe thin-film quantum dot composites are novel materials incorporating CdSe nanocrystals in a ZnSe semiconductor matrix.[2] Since the luminescence wavelength is characteristic of the imbedded quantum dots, it is adjustable in a large spectral window ∼1.8−2.5 eV. The ZnSe semiconductor matrix is expected to provide electronic passivation of the CdSe surface. Moreover, the electronic properties of the composites, e.g., electrical conductivity, may be controlled by doping the matrix, and the materials are suitable for integration into optoelectronic device structures from both electronic and processing considerations.

Electrospray organometallic chemical vapor deposition (ES-OMCVD) is a new technique for the synthesis of thin films of quantum dot composites.[2] In this technique, the films are prepared by co-deposition of ex-situ formed nanocrystals with a matrix grown by OMCVD. The nanocrystals, initially dispersed in an organic solvent, are transferred into the deposition zone of an OMCVD reactor with electrospray.[3] Although initial experiments with ES-OMCVD demonstrated the potential of the technique for the synthesis of luminescent CdSe/ZnSe quantum dot composites, the emission yield was low and degraded with increasing deposition temperatures.[2] High-resolution transmission electron microscopy (HRTEM) and scanning transmission electron microscopy (STEM) investigations of the composites revealed extensive agglomeration of the nanocrystals in the films and the presence of matrix grain boundaries at the CdSe−ZnSe interface. These defects are likely the reason for the low photoluminescence yield and the poor thermal stability of the materials. Liu et al.[4] reported a similar degradation of photoluminescence properties of silicon-based quantum dot composites.

In this report we describe a new approach to ES-OMCVD synthesis of luminescent CdSe/ZnSe quantum dot composites, relying on passivation of the CdSe nanocrystals prior to their incorporation into the host matrix. The passivation is accomplished with a thin layer of ZnSe grown on the nanocrystals prior to the ES-OMCVD synthesis. A precedent for such passivation can be found in recent reports on layered semicon-

[†] Department of Chemistry.
[‡] Department of Chemical Engineering and Materials Science and Engineering.
[§] Present address: Applied Materials, 3100 Bowers Avenue, MS 0205, Santa Clara, CA 94054
[⊥] Present address: IBM T. J. Watson Research Center, P.O. Box 218, Yorktown Heights, NY 10598
[⊗] Abstract published in *Advance ACS Abstracts,* November 15, 1995.

(1) For recent reviews see: (a) Brus, L. E. *Appl. Phys. A* **1991**, *53*, 465. (b) Wang, Y.; Herron, N. *J. Phys. Chem.* **1991**, *95*, 525. (c) Bawendi, M. G.; Steigerwald, M. L.; Brus, L. E. *Annu. Rev. Phys. Chem.* **1990**, *41*, 477. (d) Weller, H. *Angew. Chem., Int. Ed. Engl.* **1993**, *32*, 41. (e) Brus, L. E. *J. Phys. Chem.* **1994**, *98*, 3577.

(2) (a) Danek, M.; Jensen, K. F.; Murray, C. B.; Bawendi, M. G. *Appl. Phys. Lett.* **1994**, *65*, 2795. (b) Danek, M.; Jensen, K. F.; Murray, C. B.; Bawendi, M. G. *J. Cryst. Growth* **1994**, *145*, 714.

(3) (a) Fenn, J. B.; Mann, M.; Meng, C. K.; Wong, S. T.; Whitehouse, C. M. *Science* **1989**, *246*, 64. (b) Fenn, J. B. *J. Am. Soc. Mass Spectrom.* **1993**, *4*, 524. (c) Gomez, A.; Tang, T. *Phys. Fluids* **1994**, *6*, 404.

(4) Liu, X.; Wu, X.; Bao, X.; He, Y. *Appl. Phys. Lett.* **1994**, *64*, 220.

0897-4756/96/2808-0173$12.00/0

ductor particles, e.g., ZnS on CdS,[5] ZnS on CdSe,[6] CdS on HgS,[7] and SiO_2 on Si.[8] Here we describe a new solution procedure for overgrowth of CdSe nanocrystals with ZnSe using organometallic precursors. This procedure yields high-quality CdSe/ZnSe particles which can be easily purified and derivatized to be compatible with the OMCVD chemistry of the ZnSe matrix.[9] The structure and optical properties of the passivated particles in solution are probed to assess the influence of the ZnSe overlayer on the luminescent properties of CdSe nanocrystals. The overcoated CdSe nanocrystals are subsequently employed in the synthesis of CdSe/ZnSe composites by ES-OMCVD, and the photoluminescence characteristics of the materials are compared to those obtained with composites containing bare nanocrystals.

Experimental Section

Materials. Hexane (HPLC grade, Mallinckrodt), methanol (electronic grade, Mallinckrodt), butanol (Mallinckrodt), pyridine (anhydrous, Aldrich), acetonitrile (anhydrous, Aldrich), trioctylphosphine (TOP, Fluka), nonane (anhydrous, Aldrich), and selenium (electronic grade, Aezar) were used as received. Diethylzinc (DEZn, Aldrich) was filtered through a 0.2 μm PTFE filter, and dimethylcadmium (Organometallics, Inc.) was vacuum transferred prior to use. A 1.0 M stock solution of trioctylphosphine selenide was prepared as described in the literature.[10] Hydrogen carrier gas (ultrahigh purity, Matheson) was purified in a palladium cell. The OMCVD precursors, hydrogen selenide (electronic grade, Solkatronic) and DEZn (electronic grade, Texas Alkyls) were used as received.

Synthesis of CdSe/ZnSe Nanocrystals. CdSe nanocrystals of selected size were prepared by controlled growth of CdSe nuclei in a trioctylphosphine−trioctylphosphine oxide (TOP/TOPO) mixture according to a previously described procedure.[10] The nanocrystals were purified by repeated precipitation with methanol and redispersion in hexane. The width of the initial size distribution of the purified sample was narrowed by size-selective precipitation from hexane/methanol mixtures.[10]

Overgrowth of CdSe nanocrystals with a ZnSe layer was carried out in TOP under Ar using a Schlenk line technique. In a standard procedure, a sample containing ~100 mg of purified and size-selected CdSe nanocrystals was precipitated with methanol; the nanocrystals were separated in a centrifuge and transferred into a glovebox. The nanocrystals were redispersed in 10 mL of TOP containing 0.5 mmol of trioctylphosphine selenide (TOPSe). If necessary, a small amount of anhydrous nonane was added to the slurry to accelerate redispersion of the nanocrystals. The dispersion was filtered with a 0.2 μm PTFE filter, transferred into a flask backfilled with Ar, and heated to 150 °C. In a glovebox, equimolar amounts of DEZn and TOPSe were mixed in 10 mL of TOP and filtered with a 0.2 μm PTFE syringe filter (**Caution**: DEZn is highly pyrophoric!). The solution of ZnSe precursors was continuously dosed at a flow rate of ~0.3 mL/min to the heated and stirred dispersion using a syringe pump. The overgrowth of ZnSe was followed by UV/vis absorption spectroscopy. After addition of the desired amount of the precursors, the reaction mixture was cooled to room temperature. A small amount of butanol (~5 mL) was added to the reaction mixture to alcoholyze unreacted DEZn. The overcoated nanocrystals were precipitated from the mixture with hexane and separated by centrifugation. Repeated redispersion of the sample in pyridine and precipitation with hexane was used to purify the CdSe/ZnSe particles and to derivatize the surface with pyridine.[10] The nanocrystals were stored dispersed in anhydrous pyridine under nitrogen.

Preparation of the Nanocrystal Dispersions for ES-OMCVD. Pyridine-capped CdSe or CdSe/ZnSe nanocrystals were precipitated with hexane, separated on a centrifuge, and transferred into a glovebox. The nanocrystals were redispersed in anhydrous pyridine and filtered with a 0.2 μm PTFE filter. The concentration of CdSe was adjusted to ~3 mg/mL. Before the ES-OMCVD synthesis, the dispersion was diluted with a 2-fold excess of anhydrous acetonitrile and the mixture was degassed by several thaw−pump−freeze cycles on a high vacuum line. Dilution with acetonitrile was necessary for steady operation of the electrospray. Manipulation of nanocrystal dispersions was carried out on a custom-made liquid-handling system attached to the ES-OMCVD reactor.

ES-OMCVD Synthesis. The ES-OMCVD system used for the synthesis of the composites is described elsewhere.[2a] Composite films were deposited on degreased glass substrates (microscope slides, Fisher) at temperatures ranging from 150 to 270 °C. Hydrogen selenide (20 μmol/min) and DEZn (1 μmol/min), carried in hydrogen gas, were used as the matrix precursors. The electrospray atomization of the nanocrystal dispersions was carried out at 4.5 kV (dc), imposed between a capillary electrode (positive polarity) and ring counterelectrode (ground). The capillary electrode was fed with the nanocrystal dispersion at a flow rate of 17 μL/min using a syringe pump. The aerosol was carried into the growth zone of the ES-OMCVD reactor in a stream of 1000 standard cm^3/min (sccm) of hydrogen. The reactor and electrospray pressure was maintained at 600 Torr. The deposition was initiated by growth of a ZnSe film (thickness ~0.1 μm), followed by deposition of the composite (thickness ~1 μm), and finally terminated by growth of a ZnSe capping layer (thickness ~0.1 μm). This sandwich structure ensured that all the deposited nanocrystals were buried within the ZnSe matrix.

Optical Characterization. UV/vis absorption spectra were measured on a Hewlett-Packard 8452 diode array spectrometer. Photoluminescence and photoexcitation spectra were obtained on a Spex Fluorolog-2 spectrometer with front face collection. The spectra were corrected for the response of the PMT and spectral flux of the excitation source using experimentally determined correction factors. The absolute photoluminescence yields were estimated by comparing the integrated emission intensities of the particles in a pyridine dispersion with the integrated intensity for rhodamine 590 in methanol. The low-temperature photoluminescence measurements on the composites films were carried out in a Janis cryostat cooled with liquid helium. The relative photoluminescence yields for the composite films were determined from band-edge emission intensities. The absorption of the excitation light was estimated from the intensity of the transmitted light as measured on the backside of the samples with an Oriel silicon photodiode.

Chemical Composition. The Zn/Cd ratios in the ZnSe/CdSe nanocrystals and composite films were determined on an X-ray fluorescence spectrometer using a Diano V generator (Cr anode) and a HNU Si:Li detector. Samples of nanocrystals were prepared by evaporation of a few droplets of a pyridine dispersion of nanocrystals on a silicon wafer. ZnSe films grown by OMCVD in our laboratory and CdSe powder (99.99%, Alfa) were used as standards. Auger electron spectra of the nanocrystals were measured on a Perkin-Elmer AES microprobe Model 660 with a primary beam energy of 5 keV.

Electron Microscopy. High-resolution transmission electron microscopy (HRTEM) images were obtained on a Topcon

(5) Youn, H. C.; Baral, S.; Fendler, J. H. *J. Phys. Chem.* **1988**, *92*, 6320.
(6) Kortan, A. R.; Hull, R.; Opila, R. L.; Bawendi, M. G.; Steigerwald, M. L.; Carroll, P. J.; Brus, L. E. *J. Am. Chem. Soc.* **1990**, *112*, 1327.
(7) (a) Hässelbarth, A.; Eychmüller, A.; Eichberger, R.; Giersig; M.; Mews, A.; Weller, H. *J. Phys. Chem.* **1993**, *97*, 5333. (b) Mews, A.; Eychmüller, R.; Giersig, M.; Schooss, D.; Weller, H. *J. Phys. Chem.* **1994**, *98*, 934.
(8) (a) Littau, K. A.; Szajowski, P. J.; Muller, A. J.; Kortan, A. R.; Brus, L. E. *J. Phys. Chem.* **1993**, *97*, 1224. (b) Wilson, W. L.; Szajowski, P. J.; Brus, L. E. *Science* **1993**, *262*, 1242. (c) Warwa, E.; Seraphin, A. A.; Chiu, L. A.; Zhou C.; Kolenbrander K. D. *Appl. Phys. Lett.* **1994**, *64*, 1821. (d) Chiu, L. A.; Seraphin, A. A.; Kolenbrander K. D. *J. Electron. Mater.* **1994**, *23*, 347.
(9) Wright, P. J.; Cockayne, B.; Oliver, P. E.; Jones, A. C. *J. Cryst. Growth* **1991**, *108*, 525.
(10) Murray, C. B.; Norris, D. J.; Bawendi, M. G. *J. Am. Chem. Soc.* **1993**, *115*, 8706.

EM002B microscope operating at 200 kV. The nanocrystal specimens were prepared by placing a drop of a diluted pyridine dispersion on nickel/carbon TEM grids and rinsing excess dispersion with solvent after a short contact time. The samples were overcoated with a carbon film to improve the stability of the samples in the electron beam of the microscope.

X-ray Diffraction. X-ray diffraction spectra of the nanocrystals were obtained on a Rigaku 300 rotating anode diffractometer operating in the Bragg configuration using Cu Kα radiation. Specimens were prepared by spreading a thin layer of precipitated nanocrystals onto a (100) silicon wafer.

Results and Discussion

Synthesis. Recent studies have shown that a crystalline overlayer of a compound semiconductor may be formed on semiconductor nanocrystals, either by heterogeneous nucleation (precipitation), or by ion displacement reactions.[6,7,11,12] The former technique is more suitable for the combination CdSe(core)−ZnSe(shell), since the displacement reaction

$$Zn^{2+}(aq) + CdSe(s) \leftrightarrow Cd^{2+}(aq) + ZnSe(s)$$

is thermodynamically unfavorable ($\Delta G° = 56.0$ kJ/mol). Hoener et al.[13] prepared CdSe/ZnSe particles by overgrowth of CdSe seeds with ZnSe using an inverse micelle technique, demonstrating a shell-core structure of the particles by X-ray photoemission and Auger electron spectroscopy. However, the CdSe particles produced by this technique had poor optical properties caused by the presence of structural defects, and a broad particle size distribution. Murray et al.[10] described an alternative procedure for the synthesis of CdE (E = S, Se, Te) nanocrystals, relying on controlled growth of the particles at elevated temperature in a coordinating solvent. High optical quality CdSe nanocrystals, obtained with this procedure, were used as the starting material for synthesis of CdSe/ZnSe particles.

CdSe/ZnSe particles were prepared by overgrowth of size-selected CdSe nanocrystals with ZnSe in trioctylphosphine (TOP) at temperatures of 150−160 °C. Overgrowth was controlled by the delivery of the ZnSe precursors, trioctylphosphine selenide (TOPSe) and diethylzinc (DEZn), into the reaction mixture. This precursor chemistry has recently been demonstrated to have the potential for producing high quality ZnSe epilayers.[14] To avoid homogeneous nucleation of ZnSe, a slow, steady dosing of the precursors was maintained during the overgrowth.

UV/vis absorption spectra of the reaction mixture at various stages of the overgrowth are shown in Figure 1. The dosing of the ZnSe is accompanied by a dramatic increase of absorption in the UV. This effect is consistent with formation of ZnSe on the CdSe surface which is further supported by the following observations. First, in a comparative experiment without the presence of CdSe nuclei, the ZnSe precursors react slowly, yielding a white precipitate soluble in hexane. The characteristic absorption spectrum, with a sharp band at 320 nm, indicates that products might be a ZnSe analogue of the ∼1.5 nm clusters of CdS[15] and CdSe.[10] In the presence of CdSe nanocrystals, the formation of this side product is *not* observed.

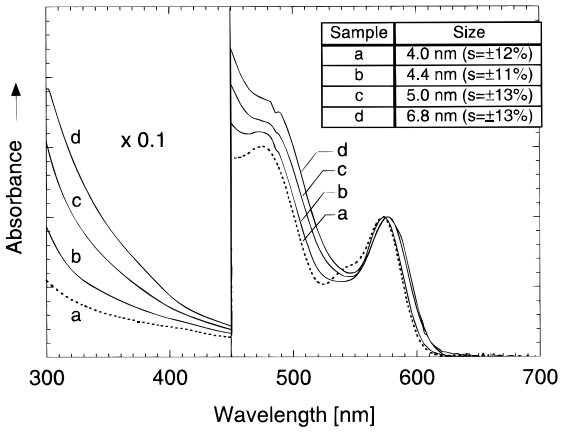

Figure 1. Evolution of the UV/vis absorption spectra of the reaction mixture during overgrowth of ∼4.0 nm CdSe nanocrystals with ZnSe. The inset shows the corresponding particle size in the reaction mixture as determined with HRTEM.

Second, the band-edge absorption of the initial CdSe nanocrystals remains nearly constant during the growth. Only a small red shift (∼2 nm) of the lowest ($1S_{3/2}1S_e$) absorption maximum can be observed after a short reaction period. A comparative experiment without dosing DEZn into the reaction mixture showed that this shift was not caused by growth of the CdSe particles via Ostwald ripening. At higher reaction temperatures (∼200 °C), a small blue shift (∼2 nm) of the $1S_{3/2}1S_e$ absorption maximum can be observed in the initial stage of the overgrowth, followed by the red shift. This effect is consistent with alloying at the CdSe/ZnSe interface. Thus, the $1S_{3/2}1S_e$ absorption band provides a sensitive probe for monitoring the integrity of the CdSe nuclei during the overgrowth process.

Third, the evolution of particle sizes in the reaction mixture was determined with HRTEM (inset of Figure 1). As expected for a heterogeneous growth mechanism, the increase in UV absorption is accompanied by an enlargement of the average particle size from 4.0 nm to 6.8 nm. The standard deviation (s) of the size distribution increased from an initial ∼10% to 13%. HRTEM images revealed that the particle shape changes from the nearly spherical morphology of the initial nanocrystals to a slightly irregular shape with an aspect ratio of ∼1.3 for ∼6.8 nm particles (Figure 2). The increase in particle size is consistent with the ZnSe/CdSe stoichiometry, as determined by X-ray fluorescence analysis. These observations further support the overgrowth mechanism, as opposed to formation of separate ZnSe particles.

The described technique allows synthesis of composite particles as large as ∼7 nm. Above this size the TOP dispersion is not stable, and the particles precipitate out of the reaction mixture preventing a uniform overgrowth. The solution properties of the overgrown particles vary with the particle. For example, while small particles (∼4−5 nm) are fairly dispersible in

(11) (a) Zhou, H. S.; Honma, I.; Koimyama, H.; Haus, J. W. *J. Phys. Chem.* **1993**, *97*, 895. (b) Zhou, H. S.; Sasahara, H.; Honma, I.; Komiyama, H.; Haus, J. W. *Chem. Mater.* **1994**, *6*, 1534.

(12) Henglein, A *Chem. Rev.* **1989**, *89*, 1861.

(13) Hoener, C. F.; Allan, K. A.; Bard, A. J.; Champion, A.; Fox, M. A.; Mallouk, T. E.; Webber, S. E.; White, J. M. *J. Phys. Chem.* **1992**, *96*, 3812.

(14) Danek, M.; Huh, J. S.; Foley, L.; Jensen, K. F. *J. Cryst. Growth*, **1994**, *145*, 530.

(15) Herron, N.; Calabrase, J. C.; Farneth, W. E.; Wang, Y. *Science* **1993**, *259*, 1426.

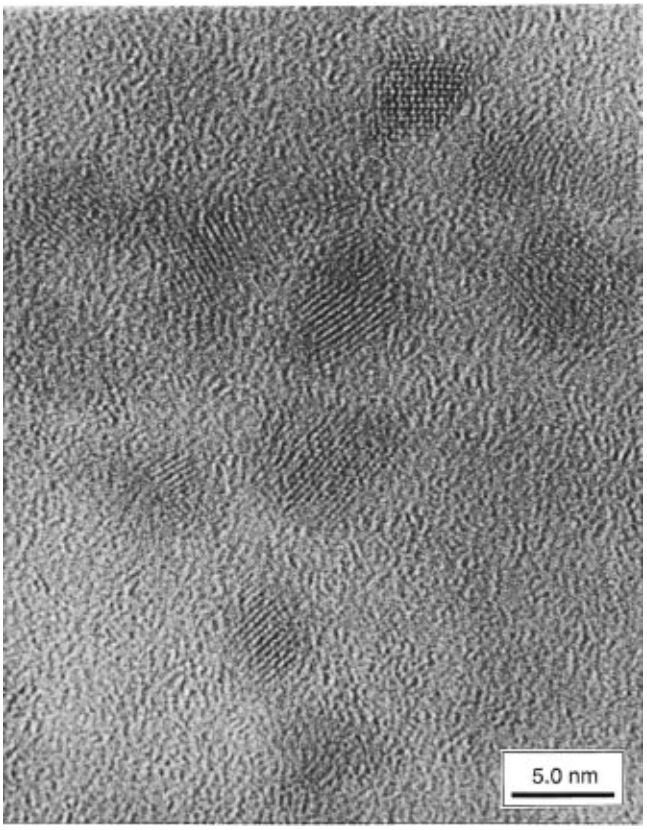

Figure 2. HRTEM images of CdSe nanocrystals overcoated with ZnSe. The [ZnSe/CdSe] ratio is ~2.5.

hexane, large particles (>5 nm) precipitate almost quantitatively after addition of hexane to the TOP dispersion. However, the precipitated particles may be readily redispersed in pyridine. A combination of low dispersibility in hexane and high dispersibility in pyridine permits isolation and purification of the composite particles from the reaction side products and unreacted TOPSe. During this purification, the TOP surface layer (cap) is quantitatively exchanged for a pyridine cap; the phosphorus content of the purified particles is below the detection limit of Auger electron spectroscopy (AES). The solubility properties of the composite particles exposed to air change over time, indicating susceptibility of the ZnSe surface to oxidation. Nevertheless, dispersions in anhydrous pyridine may be stored under an inert gas for several months without any precipitation or changes in UV/vis absorption.

Structural Characterization. High-magnification TEM images of derivatized particles with [ZnSe/CdSe] = 2.5 are shown in Figure 2. The images show well-resolved diffraction fringes of the particle lattice. The coherence of the fringes, as seen on some of the particles, is consistent with epitaxial overgrowth of ZnSe on the CdSe surface. However, the images do not provide any significant evidence as to the location of the CdSe/ZnSe interface. Some of the particles display a lack of diffraction contrast on the periphery, which might indicate the presence of an amorphous, or disordered ZnSe overlayer on the CdSe nuclei.

The crystallinity of the derivatized particles was further probed by X-ray diffraction. Figure 3 displays powder diffraction patterns of ~6.8 nm particles ([ZnSe/CdSe] = 2.5) and ~4.0 nm CdSe nanocrystals. The patterns of the composite particles consists of rather

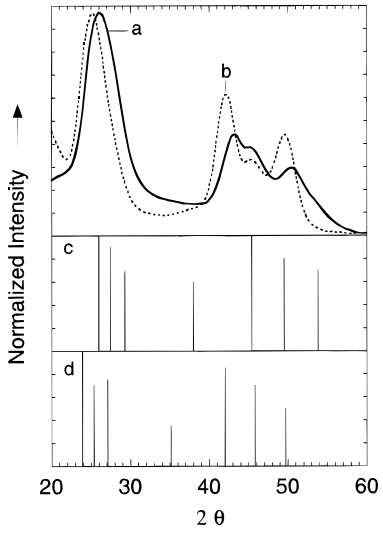

Figure 3. X-ray powder diffraction patterns of ~6.8 nm CdSe/ZnSe particles (a), ~4.0 nm CdSe nanocrystals (b), and powder diffraction lines of wurtzite ZnSe (c) and wurtzite CdSe (d). The [ZnSe/CdSe] ratio for the overcoated particles is ~2.5.

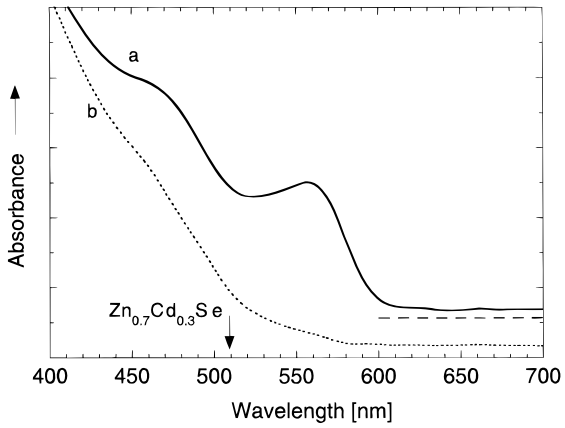

Figure 4. Room-temperature optical absorption spectra of a film of CdSe/ZnSe particles with [ZnSe/CdSe] = 2.5 before (a) and after (b) annealing in He at ~450 °C. The calculated bandgap energy for $Zn_{0.7}Cd_{0.3}Se$ bulk is shown.

broad features that do not overlap with the diffraction lines of wurtzite ZnSe or wurtzite CdSe. Such a diffraction pattern could be expected from largely alloyed particles. However, the alloying effect may be ruled out on the basis of an annealing experiment with a thin film of the overcoated particles. The absorption spectrum of the film, as deposited from solution on a glass slide, is shown in Figure 4. After ~30 min of annealing at ~400 °C in a flux of He, conditions sufficient for extensive alloying of the composite particles, the absorption edge of the film moved into a short wavelength region, as expected for a ternary alloy with the Zn/Cd stoichiometry of the original particles. The X-ray patterns, therefore, cannot be interpreted in terms of alloying. Detailed simulation of X-ray patterns from the overcoated nanocrystals will be needed to fully understand the origin and shape of the diffraction peaks.

The broad diffraction features of the overcoated particles indicate a poor crystallinity of the ZnSe overlayer. This explanation is consistent with the observation of structural disorder in the periphery region of some of the particles. However, a broadening of the diffraction spectra could also be expected for a highly

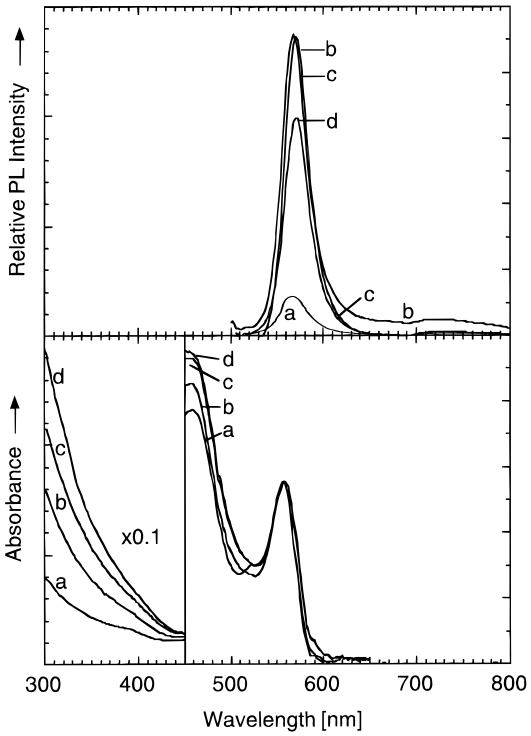

Figure 5. Room-temperature optical absorption and scaled photoluminescence spectra of CdSe (a) and CdSe/ZnSe particles with [ZnSe/CdSe] ratio of 3.6 (b), 4.3 (c), and 4.8 (d) in pyridine. The photoluminescence yields were $\phi \sim 0.05\%$ (a), 0.4% (b), 0.4% (c), and 0.3% (d). The excitation wavelength for the photoluminescence was 480 nm.

crystalline overlayer of ZnSe with variations in the lattice spacing induced by the lattice mismatch.[11a]

The shell-core structure of the passivated particles was probed qualitatively through a combination of AES and X-ray fluorescence analysis.[6,13] AES is sensitive to surface composition because of the short escape depth for Auger electrons (~1.0 nm), whereas X-ray fluorescence allows analysis of the overall composition of the particles. For particles with a core size ~3.5 nm and overall [ZnSe/CdSe] = 4.8, AES analysis of the sample gave [ZnSe/CdSe] = 7.0. This ratio is low for a symmetrical shell-core structure with a ~1.3 nm thick overlayer, indicating that the overlayer is not uniform around the CdSe core.

Optical Characterization. The effect of passivation on the optical properties of CdSe dots was explored with a set of samples isolated from a single preparation at various stages of the overgrowth. Prepared from identical CdSe nanocrystals, these samples allowed observation of the true changes in the optical properties of the particles as a function of the [ZnSe/CdSe] ratio.

Room-temperature absorption spectra of purified CdSe nanocrystals and CdSe/ZnSe particles, with [ZnSe/CdSe] ratios ranging from 3.6 to 4.8, are shown in Figure 5. All the spectra display a similar absorption edge shape. The $1S_{3/2}1S_e$ absorption maximum undergoes a slight red shift (~4 nm) after deposition of a ZnSe layer on the CdSe surface. The decrease of the exciton energy is consistent with relaxation of quantum confinement in the CdSe dots due to the presence of ZnSe on the CdSe surface. The surface derivatization is also accompanied by the disappearance of the second absorption band in the valley of the absorption edge. The second excited state has more electron density close to the particle surface and, therefore, its energy should be more sensitive to surface derivatization.[16] The dramatic increase in absorption in the short wavelength region with increasing [ZnSe/CdSe] ratio suggests that some portion of the high-energy optical transitions are localized in the ZnSe layer.

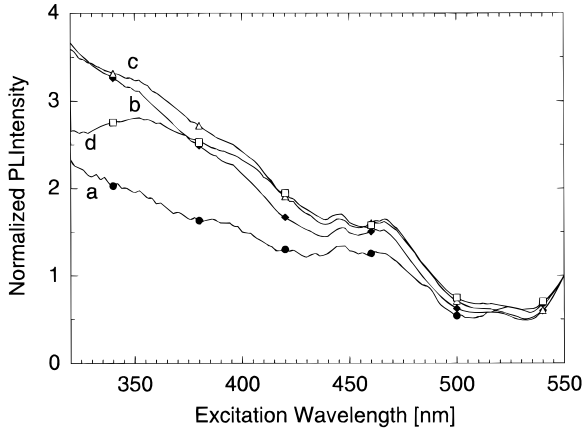

Figure 6. Room-temperature photoluminescence excitation spectra of CdSe (a, ●) and CdSe/ZnSe particles with [ZnSe/CdSe] ratio of 3.6 (b, ◆), 4.3 (c, △), and 4.8 (d, □) in pyridine. The emission was detected at 570 nm and the spectra are normalized to the intensity at 550 nm.

Photoluminescence spectra of bare and passivated particles are also shown in Figure 5. The spectra, scaled by the photoluminescence yield (ϕ), display sharp band-edge emission and weaker, broad luminescence originating from deep electronic traps. The presence of the passivating layer results in a small red shift (~2−4 nm) of the band-edge emission of CdSe nanocrystals, consistent with the shift of the band-edge absorption. The same Stokes shift (~10 nm) of the band-edge emission is observed for both bare and overcoated particles. The width of the emission band is identical for all particles, providing further evidence that the CdSe dots preserve their initial size distribution during passivation. There is, however, a significant difference in the photoluminescence yield between the bare and passivated nanocrystals. The yield of band-edge emission from the bare particles capped with pyridine is very low ($\Phi \sim 0-0.05\%$), whereas the photoluminescence yield for the overcoated particles is ~0.3−0.4%. This result is consistent with observations of enhanced band-edge emission from CdSe(core)−ZnS(shell)[6] and CdS(core)−HgS(shell)−CdS(shell)[7b] particles. The absolute photoemission yield for the overcoated particles is low compared to $\Phi \sim 10\%$ for CdSe nanocrystals capped with TOP/TOPO,[10] which is not surprising in view of the structural characterization of the particles. Defects in the overlayer and at the CdSe−ZnSe interface should be effective recombination centers for the exciton. Thus, it is likely that the observed band-edge photoluminescence originates from the small fraction of particles with a defect-free overlayer.

The effect of passivation on the emission properties of the nanocrystals was further probed by photoluminescence excitation spectroscopy. The room temperature excitation spectra of bare and overcoated particles, displayed in Figure 6, are normalized to the excitation

(16) Norris, D. J.; Bawendi, M. G. Measurement and assignment of the size dependent optical spectrum in CdSe quantum dots, submitted.

efficiency at 550 nm, a wavelength predominantly absorbed by the CdSe core. Thus, the normalized spectra allow a direct comparison of the photoexcitation efficiency with the corresponding absorption spectra in Figure 5. The photoexcitation spectra show an increase of excitation efficiency in the short-wavelength region for the overcoated particles due to the absorption in the overlayer. This result provides additional evidence of the presence of ZnSe on the CdSe surface, since energy transfer between separated particles in the dispersion would be unlikely. If the ZnSe and CdSe particles were separated, the ZnSe phase would be an "internal" filter for the short-wavelength excitation light and the photoexcitation efficiency would drop dramatically. Moreover, the spectra indicate low defects at the ZnSe−CdSe interface in at least a significant fraction of the particles, since transfer of photogenerated carriers to CdSe can compete with nonradiative recombination within the ZnSe overlayer. However, the excitation efficiency does not increase monotonically with the increase of the absorptivity in the blue and near-UV spectral regions. The spectrum for particles with [ZnSe/CdSe] = 4.8 suggests that the efficiency drops for too thick an overlayer. This peculiar dependence on the [ZnSe/CdSe] ratio can be explained in terms of an increasing number of structural defects in the overlayer with increasing layer thickness caused by the lattice mismatch. This interpretation is consistent with the relaxation of the lattice mismatch in strained CdSe/ZnSe superlattices via formation of misfit dislocations.[17] Formation of lattice defects in CdSe quantum wells above the critical thickness of ~4 monolayers have been reported to deteriorate photoluminescence characteristics of CdSe/ZnSe superlattices.

On the basis of the present results, we believe that further improvement of the photoemission yield from the passivated CdSe is possible by optimizing the passivation procedure. The crystalline quality of the CdSe−ZnSe interface and the coherence of the overlayer might be improved by annealing in a coordinating solvent.[18]

Synthesis of CdSe/ZnSe Thin-Film Composites with Passivated CdSe Dots. Thin-film composites incorporating the overcoated nanocrystals in a ZnSe matrix were prepared by ES-OMCVD,[2] as described in the Experimental Section. Reference samples of composite films incorporating bare CdSe nanocrystals were also prepared under identical deposition conditions. The effect of the preformed ZnSe overlayer on the luminescent properties of the composites was probed by photoluminescence spectroscopy at room temperature and 10 K. Room-temperature spectra of the thin-film composites prepared from bare and overcoated CdSe nanocrystals at various substrate temperatures are shown in Figure 7.

Spectra for the bare CdSe nanocrystals consist of a weak band-edge emission and a dominant deep-level emission. The wavelength of the band-edge emission

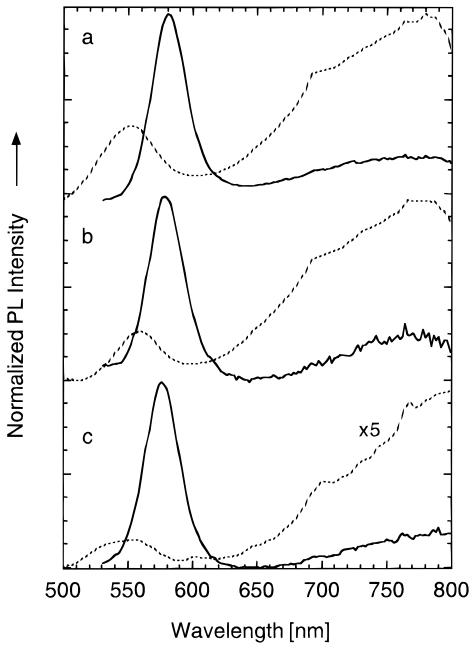

Figure 7. Room-temperature photoluminescence spectra of CdSe/ZnSe composite films with bare (dotted line) and overcoated (solid line) ([ZnSe/CdSe] = 0.4) CdSe quantum dots synthesized by ES-OMCVD at substrate temperatures of 150 (a), 200 (b), and 250 °C (270 °C for overcoated) (c). The excitation wavelength was 480 nm. The wavelength corresponding to maximum luminescence differs slightly between experiments because of minor variations in nanocrystallite sizes.

is characteristic of the size of the initial CdSe nanocrystals.[2] The maximum of the band-edge emission undergoes a ~10 nm red shift with increasing deposition temperature from 150 to 200 °C. A further increase of the temperature to 250 °C moves the emission wavelength back to ~550 nm. Similar changes in the emission wavelength with deposition temperature were also observed in photoluminescence spectra of composites incorporating nanocrystals of a different size. Scanning TEM on composite samples revealed that a large fraction of the incorporated nanocrystals are in an agglomerated form[2a] and the red shift for deposition temperature of ~200 °C is consistent with growth of the agglomerated particles and energy transfer to the larger particles in the agglomerate. The blue shift at higher temperatures (~250 °C) indicates alloying at the CdSe−ZnSe interface. At the same time, the relative yield of the band-edge emission drops by 1 order of magnitude. The predominance of deep-level emission, originating from electronic traps at the CdSe surface, is consistent with the presence of structural defects at the dot interface, as observed by HRTEM.[2]

Incorporation of overcoated nanocrystals results in a remarkable enhancement of the photoluminescence properties of the materials. The room-temperature spectra (Figure 7) are now dominated by an intense band-edge emission. The widths of the emission bands are comparable to those for the initial nanocrystals. The increasing deposition temperature results in a ~4 nm blue shift of the emission maximum, which is consistent with alloying at the CdSe/ZnSe interface. The deep-level emission remains weak even for composite deposited at ~270 °C. The insensitivity of deep-level emission to processing conditions suggests that the deep-level

(17) Recent papers include: (a) Zajicek, H.; Juza, P.; Abramof, E.; Pankratov, O.; Sitter, H.; Helm, M.; Brunthaler, G.; Faschinger, W.; Lischka, K. *Appl. Phys. Lett.* **1993**, *62*, 717. (b) Zhu, Z.; Yoshihara, H.; Takebayashi, K.; Yao, T. *Appl. Phys. Lett.* **1993**, *63*, 1678. (c) Zhu, Z.; Yoshihara, H.; Takebayashi, K.; Yao, T. *J. Cryst. Growth*, **1994**, *138*, 619. (d) Matsumoto, T.; Iwashita, T.; Sasamoto, K.; Kato, T. *J. Cryst. Growth*, **1994**, *138*, 63.

(18) Bawendi, M. G.; Kortan, A. R.; Steigerwald, M. L.; Brus, L. E. *J. Phys. Chem.* **1989**, *93*, 7282.

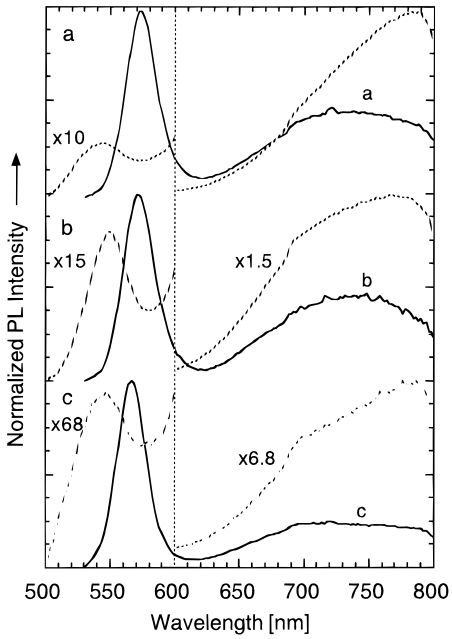

Figure 8. The 10 K photoluminescence spectra of CdSe/ZnSe composite films with bare (dotted line) and ZnSe overcoated (solid line) ([ZnSe/CdSe] = 0.4) CdSe quantum dots synthesized by ES-OMCVD at substrate temperatures of 150 (a), 200 (b), and 250 °C (270 °C for overcoated) (c). The excitation wavelength was 480 nm. The wavelength corresponding to maximum luminescence differs slightly between experiments because of minor variations in nanocrystallite sizes.

emission most likely originates from electronic traps already present in the core CdSe nanocrystals.

The 10 K spectra further accentuate the presence of deep electronic traps on the surface of the bare CdSe nanocrystals (Figure 8). The spectra are dominated by an intense and broad deep-level emission. The enhancement of the deep-level emission is consistent with a decrease in the rate of nonradiative recombination at the lower temperature. The band-edge emission remains very weak, indicating that a marginal fraction of the nanocrystals is electronically passivated by the matrix.

Band-edge emission dominates in the 10 K photoluminescence spectra (Figure 8) for the thin-film composites with overcoated nanocrystals. The intensity of the deep-level emission is increased slightly relative to the room temperature spectra. The increase of the deposition temperature from 150 to 270 °C is accompanied by an ~8 nm blue shift of the emission maximum, while the fwhm of the bands remain unchanged. This result is rather surprising since the imbedded particles experience varying exposure times during the film synthesis, depending on their depth in the composite layer (ranging from ~5 to ~60 min). Intuitively, the composites grown at a high temperature should display a broadening of the emission bandwidth due to differences in temperature history. This suggests that changes in particle characteristics are confined to the early stages of incorporation.

The room-temperature and 10 K photoexcitation spectra for the composites with bare nanocrystals shown in Figure 9 confirm the assignment of the photoluminescence spectra and provide additional insight into the optical characteristics of the composites. The excitation spectra for the band-edge emission display the absorption spectrum of the nanocrystals in the 460−520 nm range. At shorter wavelengths the excitation efficiency drops dramatically due to the absorption of excitation light in the matrix. Thus, the absorption edge of the matrix at room temperature and 10 K can be identified on the spectra. The 10 K excitation spectrum for the deep-level emission displays a maximum corresponding to the $1S_{3/2}1S_e$ absorption band of the nanocrystals. The spectrum provides clear evidence that the deep-level emission in Figure 8 originates from the CdSe dots and not from the matrix.

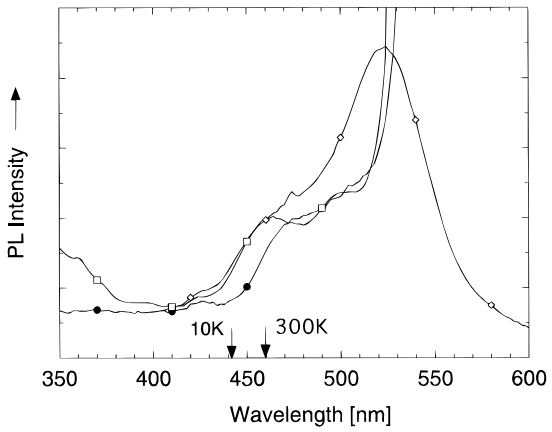

Figure 9. Room-temperature and 10 K photoluminescence excitation spectra of CdSe/ZnSe composite films with bare CdSe quantum dots synthesized by ES-OMCVD at 200 °C. The 300 K spectra were detected at 554 nm (●) and the 10 K spectra at 546 (□) and 710 nm (◇). The 300 K and 10 K bandgap of cubic ZnSe is shown with the arrows.

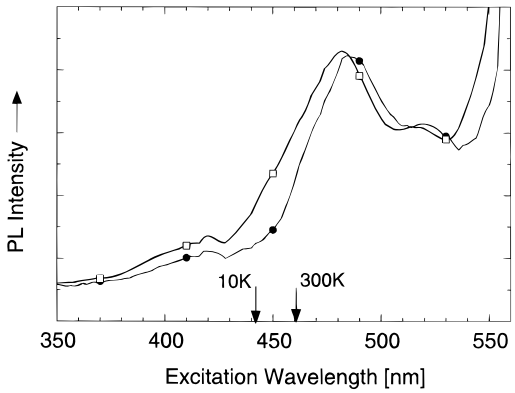

Figure 10. Room-temperature and 10 K photoluminescence excitation spectra of CdSe/ZnSe composite films with overcoated CdSe quantum dots synthesized by ES-OMCVD at 200 °C. The size of the initial CdSe dots was ~3.7 nm, [ZnSe/CdSe] = 4.0. The 300 K spectra were detected at 576 nm (●) and the 10 K spectra at 570 nm (□). The 300 and 10 K bandgap of cubic ZnSe is shown with the arrows.

The room-temperature and 10 K photoexcitation spectra for the band-edge emission for composites with overcoated dots (Figure 10) show the absorption bands of the nanocrystals in the ~480−550 nm range and the absorption edge of the matrix at the shorter wavelengths. The excitation spectra indicate that the exciton states of the dots are populated by absorption of the excitation light in the nanocrystals. A high density of recombination centers in the polycrystalline matrix, associated with structural defects and grain boundaries, does not allow population of the CdSe exciton states by excitation of the matrix. The lack of matrix photoluminescence supports this explanation.

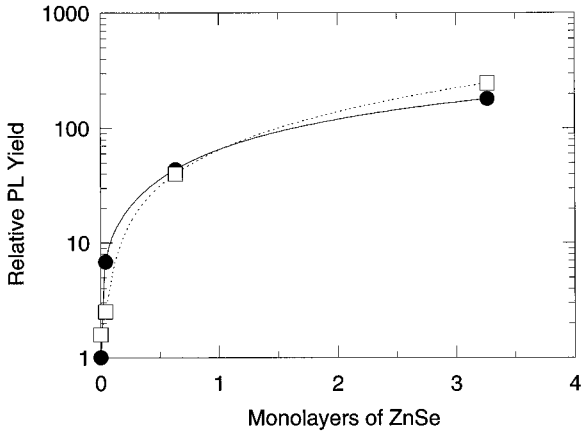

Figure 11. Relative band-edge photoluminescence yield for CdSe/ZnSe composite films with bare and passivated CdSe dots. The samples were synthesized by ES-OMCVD at substrate temperatures of 200 (●) and 260 °C (□). The number of ZnSe monolayers in the passivating layer is calculated from the [ZnSe/CdSe] stoichiometry of the composite particles, assuming a symmetrical shell−core structure. The excitation wavelength was 500 nm.

The effect of the passivation on the luminescent properties of the composites was explored further with films containing particles of varying thicknesses of ZnSe overlayer. The change in yield of the band-edge photoluminescence with the thickness of the ZnSe overlayer is shown in Figure 11 for two deposition temperatures, 200 and 260 °C. The thickness of the overlayer is calculated from the [ZnSe/CdSe] stoichiometry and the size of the initial particles, assuming a symmetrical shell−core structure. A significant enhancement of the emission yield by more than 1 order of magnitude, as compared to the composite film containing bare CdSe dots, is observed for particles passivated with a ∼0.6 monolayer of ZnSe. Deposition of ∼3 monolayers of ZnSe results in an increase of yield by a factor of ∼100. This enhancement of the photoluminescence yield, accompanied by a conversion of the deep-level emission into band-edge emission, demonstrates an effective electronic passivation of the CdSe dots with the ZnSe overlayer. For composites with overcoated dots, the photoluminescence yield is insensitive to the deposition temperature, consistent with the concept of chemical passivation of CdSe surface.

Conclusions

Electronic and chemical passivation of CdSe nanocrystals is essential for synthesis of luminescent CdSe/ZnSe thin-film quantum dot composites by ES-OMCVD. Such passivation can be accomplished by overcoating CdSe nanocrystals with a layer of ZnSe. A solution procedure, relying on heterogeneous nucleation of the passivating layer on the surface of the nanocrystals, was developed for the passivation. Thin-film quantum dot composites with the passivated nanocrystals display a remarkable enhancement of the photoluminescence quantum yield (by two orders of magnitude). The passivated nanocrystals allow synthesis of the composites at temperatures above 200 °C, the conditions required for growth of a stable crystalline matrix.

Characterization of the passivated nanocrystals revealed structural defects in the passivating layer and imperfections at the CdSe/ZnSe interface, resulting in a relatively low room-temperature photoluminescence yield ($\Phi \sim 0.4\%$). We believe that the yield can be improved significantly provided a coherent, essentially defect-free passivating layer is grown on a large fraction of the particles.

Acknowledgment. This work was supported, in part, by NSF (DMR-9157491 and DMR-9202672). The authors wish to acknowledge the assistance of Mr. Mike Frongillo with HRTEM imaging and the use of MRSEC shared facilities supported by NSF (DMR-940034). M.G.B. thanks the Lucille and David Packard Foundation and the Alfred P. Sloan Foundation for Fellowships.

CM9503137